Carbohydrate Polymers 84 (2011) 316–322

Contents lists available at ScienceDirect

Carbohydrate Polymers

journal homepage: www.elsevier.com/locate/carbpol

Structure and rheology of nanocrystalline cellulose

Dagang Liu[a,b,*], Xiaoyu Chen[c], Yiying Yue[b], Mindong Chen[a], Qinglin Wu[b]

[a] College of Chemistry, Nanjing University of Information Science & Technology, Nanjing 210044, China
[b] School of Renewable Natural Resources, Louisiana State University Agricultural Center, Baton Rouge, LA 70803, USA
[c] College of Chemistry and Chemical Engineering, Nanjing University, Nanjing 210093, China

ARTICLE INFO

Article history:
Received 23 September 2010
Received in revised form 3 November 2010
Accepted 17 November 2010
Available online 26 November 2010

Keywords:
Cellulose nanocrystal
Liquid crystal
Colloid
Porous foam

ABSTRACT

Sulfate hydrolysis and high-pressure homogenization were combined to reduce the size of microcrystalline cellulose to the nanoscale. The obtained needle-shaped nanocrystals showed a relative uniform size with length of 90 ± 50 nm and width of 10 ± 4 nm. Rheology and phase transition of the nanocrystal colloids were studied. The flowability and modulus of the colloids showed a strong relationship with frequency, temperature, and concentration of the nanocrystals. Nanocrystals self-assembled into a liquid crystal phase in colloids and even in the dried film. Structure and morphology of the ordered liquid crystalline phase were characterized by scanning electron microscope and polarized optical microscope. It was found that cellulose nanocrystals were self-aligned layer by layer, which was responsible for the color of the dried film and also allowed an ordered layered microporous foam from the freeze-dried nanocrystalline colloids.

1. Introduction

Cellulose nanocrystals (CNs) are the fundamental constitutive polymeric motifs of macroscopic cellulosic-based fibers, and are extracted as a colloidal suspension by acid hydrolysis of cellulosic materials, such as bacteria, cotton, and wood pulp. They have attracted a lot of attention not only because of their special physical and chemical properties but also due to their inherent renewability and sustainability in addition to their abundance. They have been widely employed as reinforcing agents in nanocomposites (Liu, Zhong, Chang, Li, & Wu, 2010; Liu, Liu, Yao, &Wu, 2010), electro-optical materials, biocarrier, etc., due to their low cost, availability, renewability, light weight, nanoscaled dimension, and unique morphology (Habibi, Lucia, & Rojas, 2010; Nishiyama, 2009; Siro & Plackett, 2010).

The properties of cellulose nanocrystals were closely related to their structure, size, and surface charge. For example, it is difficult to get an ordered liquid crystal materials by mechanical or enzyme methods because of the polydispersity and heterogeneity nature. Mechanical high-shear disintegration and high-pressure homogenization were used to isolate nanofibrillated cellulose (NFC) from raw commercial pulp and straw by Zimmermann et al. It was found that the treatment resulted in nano-scaled fibril networks (Zimmermann, Bordeanu, & Strub, 2010). Research from Henriksson, Henriksson, Berglund, and Lindstrom (2007) showed that the acid hydrolyzed microfibrillated cellulose (MFC) showed an inhomogeneous distribution of nanofiber geometry and a large extent of thick cell wall fragments of low aspect ratio, but enzymatically pretreated cellulosic wood fibers had a more favorable structure than nanofibers resulting from fibers subjected to hydrolysis by strong acid. However, Gray and coworkers discovered that unique self-assembled ordered liquid crystal phase was formed when the obtained cellulose crystallites were short and uniform enough (always less than 100 nm) and had a high degree of sulfate esterified onto the surface (Beck-Candanedo, Roman, & Gray, 2005; Dong, Revol, & Gray, 1998; Roman & Gray, 2005). So the chemical hydrolysis was used to prepare cellulose nanocrystalline materials possessing unique structural optical properties (Revol, Godbout, & Gray, 1998). In addition, colloidal suspensions composed of cellulosic nanocrystals or nanospheres by chemical and ultrasonic methods were reported. The suspension composed of spherical nanocrystals exhibited a liquid crystalline textures changed with varying concentration (Wang, Ding, & Cheng, 2008).

In our previous study, high pressure homogenizer was used to prepare starch nanoparticles in the water system. The starch colloids transformed from a suspension to a gel with increasing content of starch nanoparticles, accompanied with a change in zeta potential and flow properties (Liu, Wu, Chen, & Chang, 2009). In this study, chemical and homogenization treatments were combined to fabricate more uniform cellulose nanoparticles. The rheological properties of cellulose nanocrystalline suspension and gels were then characterized, and the structure and optical properties of the cellulosic nanocrystals were studied. We tried to provide a clue

* Corresponding author at: School of Renewable Natural Resources, Louisiana State University Agricultural Center, Baton Rouge, LA 70803, USA.
Tel.: +1 225 578 4251; fax: +1 225 578 4251.
E-mail address: dagangliu@gmail.com (D. Liu).

0144-8617/$ – see front matter © 2010 Elsevier Ltd. All rights reserved.
doi:10.1016/j.carbpol.2010.11.039

between cellulose microstructure and properties of the ordered nanocrystalline phase.

2. Materials and methods

2.1. Materials

Microcrystalline cellulose powder (Avicel FD-100 MCC) was provided by FMC Biopolymer (Philadephia, PA) and selected as raw materials for producing cellulose nanocrystals. Sulfuric acid (95–98 wt.%, VMR, West Chester, PA) was of analytical grade and used as received without further purification. MCC (40 g) was mixed with 64 wt.% sulfuric acid aqueous solution (700 mL) and stirred vigorously at 45 °C for 3 h. Immediately five folds dilution with water were applied to stop the hydrolysis reaction. The suspensions were then centrifuged at 12,000 rpm for 10 min (Sorvall RC-5B Refrigerated Superspeed Centrifuge, Du Pont Instrument), washed with distilled water for 4–5 times. The crystals were separated from the suspension by centrifuging after each washing. The precipitate was then placed in regenerated cellulose dialysis tubing (Fisher Scientific, Pittsburgh, PA) having a molecular weight cutoff of 12,000–14,000, and dialyzed against distilled water for several days until the pH of water reached a value of 7.0.

To further reduce the size of the cellulose crystals, mechanical treatment was applied for the chemically treated samples. The suspensions of cellulose crystals were processed through a high-pressure homogenizer (Microfluidizer M-110P, Microfluidics Corp., MA, USA) with a pair of Z-shaped interaction chambers (one 200 μm ceramic and the other 87 μm diamond) under operating pressure of 207 MPa. Suspensions passed through the interaction chambers at a rate of 133 mL/min for 10 passes. After 10 passes, the obtained sample was dried using a freeze-dryer (FreeZone, 2.5 plus, Labconco Corporation, Kansas City, MO) and thus prepared cellulose crystals were noted as CNs. Collected CNs powder was diluted into aqueous suspension with the desired concentration and then passed through the homogenizer for other two passes. The homogenized CNs colloids were placed at room temperature for one month, and became more viscous. Some selected colloids are noted as CNs-0.91, CNs-2.03, and CNs-3.17, according to their concentrations of 0.91%, 2.03% and 3.17%, respectively.

2.2. Preparation of CNs foam and liquid crystal film

The homogenized CNs colloids after storing at room temperature for one month were quickly frozen in liquid nitrogen, and then the lyophilized sample was put into a freeze-dryer for 48 h to obtain CNs foam. When the homogenized CNs suspension was poured into a polystyrene Petri dish and cast in an oven at 40 °C. After water in the colloids was slowly evaporated, a colorful solid film was obtained. Both CNs foam and film were kept in desiccators for further characterization.

2.3. Characterization

Wide-angle X-ray diffraction (WAXD) patterns of the freeze-dried CNs powder were performed on a Siemens D5000 rotating anode wide angle X-ray diffractometer with Cu Kα radiation ($\lambda = 0.154$ nm) at 40 kV and 30 mA. X-ray diffraction data were collected from $2\theta = 5^\circ$ to 40° at a scanning rate of 0.02°/min at room temperature. Diluted CNs suspensions with or without negative staining were dropped on the copper grids coated with carbon support film for observation. Negative staining involved application of ~10 μL of 2% uranyl acetate solution to the grid. In the case, excess liquid was blotted from the sample by lightly touching the edge of the grid with an edge or corner of filter paper. Negative stained samples were carried out by transmission electron microscope (TEM, JEOL 100CX) with an accelerating voltage of 80 kV. High-resolution transmission electron microscopy (HRTEM) observations of the diluted CNs suspension without staining were carried out on a JEOL JEM 2010 FEF (UHR) electron microscope with an accelerating voltage of 200 kV. Scanning electron microscopy (SEM) was performed using a Hitachi S-3600N VP SEM (Hitaschi, Japan) to investigate the morphology of the freeze-dried foam and liquid crystal film. Surface or cross-section of the nanocrystalline foam and film was coated with gold for SEM observation at 20 kV.

The rheological behavior of the colloids was investigated with a stress-imposed rheometer (AR2000, TA Instruments, GB), using a cone/plate geometry (diameter 6 cm, angle 3°59′, truncation 113 μm) for flow measurements or a plate/plate geometry for dynamic measurements (diameter 6 cm, gap 1 mm). Dynamic (or oscillatory) measurements were performed in the frequency range of 0.1–100 Hz and temperature range of 5–50 °C at a percentage strain between 1 and 5%, depending on the nanocrystalline concentration, to remain in the linear domain. A Nikon (Tokyo, Japan) MDA502AA E400 polarized optical microscope (POM) was used for liquid crystal phase observation of CNs colloids and film that were sandwiched between glass slides.

3. Results and discussion

3.1. Morphology and structure of CNs

Raw MCC particles without any treatment did not suspend but sediment in water because of the large particle size. After treatment with sulfuric acid, a suspension of hydrolyzed MCC was obtained. After a further passage through a high-pressure homogenizer, the suspension was converted into a transparent colloid with blue color. After storage for more than one month, the suspension lost its flowability and turned into viscose gel. Fig. 1(a) shows TEM micrograph of cellulose nanocrystals in the colloids. The CNs were shaped like needles with length of 90 ± 50 nm and width of 10 ± 4 nm. The histogram exhibited in Fig. 1(b) shows that most of them presented a relative uniform size with length of 60–120 nm, which would give an aspect ratio varying from 10 to 15. Thus it is shown that the combined chemical and mechanical treatment could effectively reduce the size of the cellulose crystals, which could then be dispersed to give an aqueous suspension. Fig. 1(c) shows the HRTEM micrograph of CNs, in which one bundle of fibrils was revealed to have a high level of crystal orientation from their clear lattice fringes. For the first time the lattice fringes was observed by TEM, which showed that the interplanar spacing between adjacent lattice fringes was 0.389 nm which was in accord with the (0 0 2) crystal plane of cellulose I. WAXD pattern of freeze-dried CNs in Fig. 1(d) shows a sharp strong peak at $2\theta = 22.7^\circ$, which is attributed to the (0 0 2) plane of cellulose I (Muller, Hori, Itoh, & Sugiyama, 2002; Sao, Samantaray, & Bhattacherjee, 1994). A common conclusion was achieved based on results from TEM and WAXD, that is, cellulose nanocrystals, composed of nanofibrils, exhibited cellulose I structure with crystalline orientation along C axis. It was thought that cellulose molecules located adjacent in the 0 0 2-lattice layers were bonded to one another by intermolecular hydrogen bonds between the hydroxyls on the carbon atoms C (6) and C (3) in the crystal lattice. The internal cohesion was being established by the transition of the long cellulose chain molecules to nanofibrils inside the elementary fibrils. And then the nanofibrils were parallel arranged into crystallites and crystallite strands caused by secondary valence hydrogen bonds formed by the hydroxyl groups. Our results efficiently supported those reported structure models of the native cellulose fiber (Atalla & Vanderhart, 1984; Gardner & Blackwel, 1971).

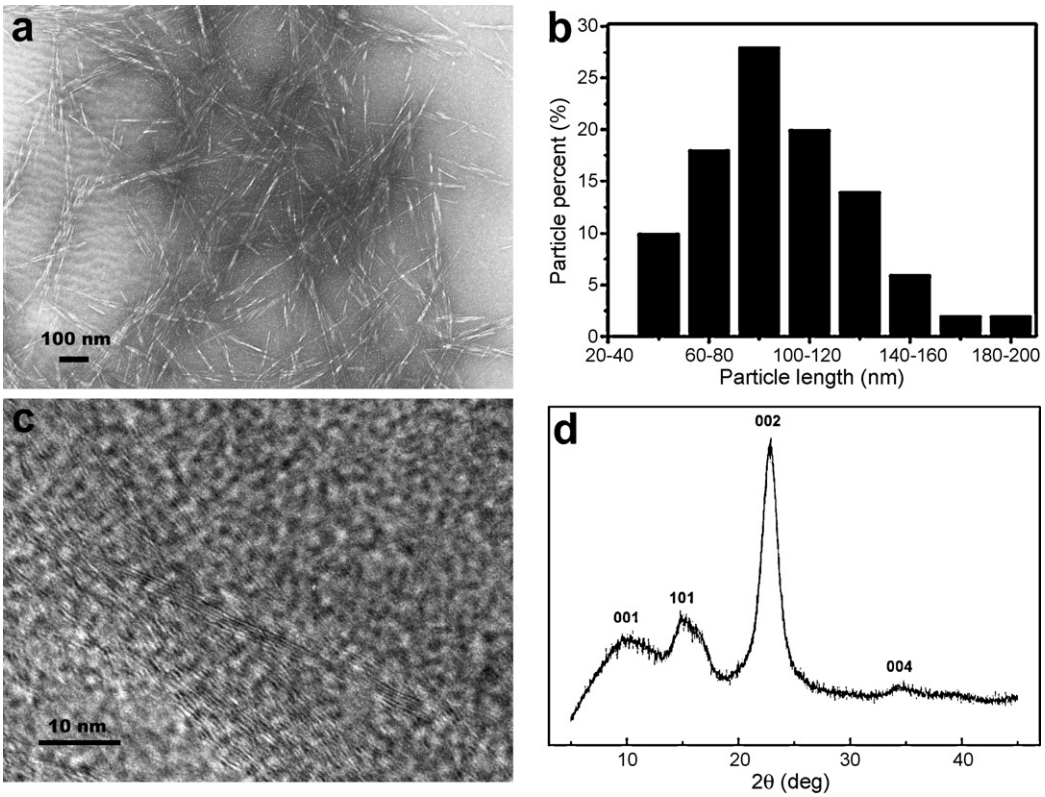

Fig. 1. TEM (a) and HRTEM (c) micrographs of CNs nanoparticles, the statistical histogram of particle size distribution (b), and the WAXD diffraction patterns of CNs (d).

3.2. Rheology and liquid crystal phase transition of CNs colloids

From suspension to gel, the colloid of CNs showed different states because of the varying of the concentration of cellulosic nanoparticles. Fig. 2 shows viscosity (η) of the CNs colloids with different concentrations as a function of shear rate ($d\gamma/dt$) at room temperature. The shear dependence of the viscosity profile showed two distinct regions. The first region was observed at lower shear rates and represented a constant decrease in the viscosity. There is a near linear relationship between the $\log(\eta)$ and $\log(d\gamma/dt)$, indicating a shear thinning behavior. At higher shear rates, a transition was occurred and the second region presented that the viscosity increased with increasing of shear rate after critical shear rate. And also the viscosity was enhanced as the concentration of CNs increased from 0.91%, to 2.03%, and to 3.17%. It was thought that network constructed by strong hydrogen or ionic bonding interactions among nanocrystals was broken by increasing shear strength at the first stage, and then the nanocrystals were rearranged to form an ordered network again, thus leading to a sudden increase in viscosity. The critical shear transition shifted to higher shear rate with increasing concentration of the CN colloids, which was dependent on hardness of the original network. However, the shear thinning behavior was observed over a wide range of shear rates (from 10^{-3} to $10^{4}\ s^{-1}$) for CNs colloids, as recognized at an early

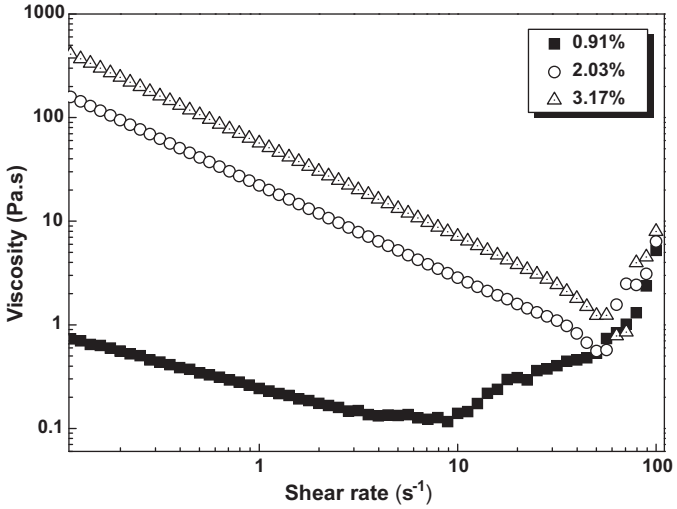

Fig. 2. Viscosity as a function of shear rate for the CNs colloids at different concentrations.

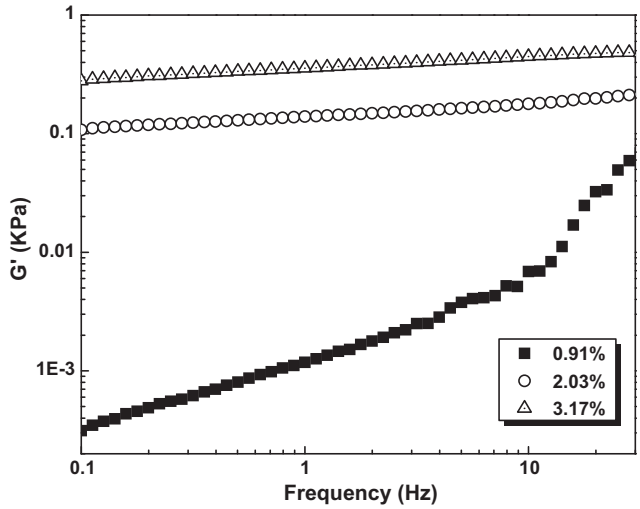

Fig. 3. Storage modulus (G') as a function of frequency for the CNs colloids at different concentrations.

stage (Bercea & Navard, 2000; Edwards & Mchugh, 1993). A plateau was reported to exist in the viscosity–shear rate curve because of the broken down of cellulose whisker domains by shearing force (Borsali & Gnanou, 2004; Onogi & Asada, 1980). CNs in this work did not follow above mentioned fluidic properties. Fig. 3 illustrates the storage modulus of CNs colloids as a function of frequency. For the suspension of CNs-0.91, the value of G' is very low. However, the G' of CNs with concentration of 3.17% was more than 0.20 kPa, which was magnitude higher than typically observed for non-entangled low-aspect-ratio cellulose I gels (Laka, Chernyavskaya, Treimanis, & Faitelson, 2000; Marsano, Bianchi, Boero, Gastaldi, & Focher, 1997). It indicated a gel-like behavior due to the high aspect ratio of the nanofibril gelation network. The storage modulus of CNs colloids was elevated either by raising concentration or frequency. Fig. 4 shows storage modulus of CNs colloids as a function of the temperature. For the colloids CNs-0.91, CNs-2.03 and CNs-3.17 showed a high relevance with temperature. A maximum G' value was obtained when the temperature reached at 35 °C in the G'/T curves, which was at least four times higher than G' at 20 °C for sample CNs-2.03 and CNs-3.17. And CNs-0.91 showed a maximum G' value at 40 °C. It was interesting and thought to be due to greater

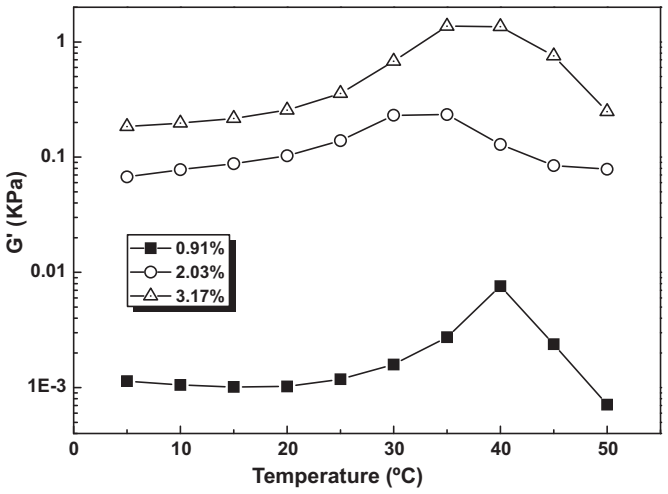

Fig. 4. Storage modulus (G') as a function of temperature at a frequency of 1 Hz for the CNs colloids at different concentrations.

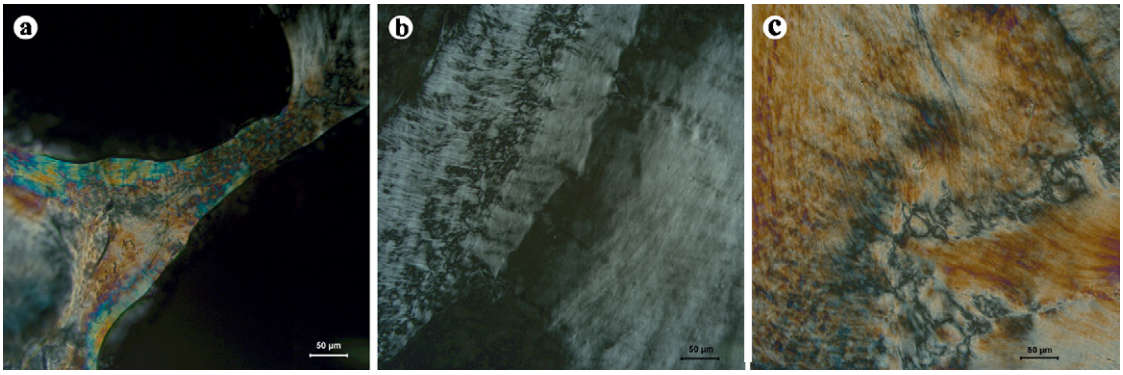

Fig. 5. POM micrographs of CNs colloids at concentration of 0.91% (a), 2.03% (b), and 3.17% (c).

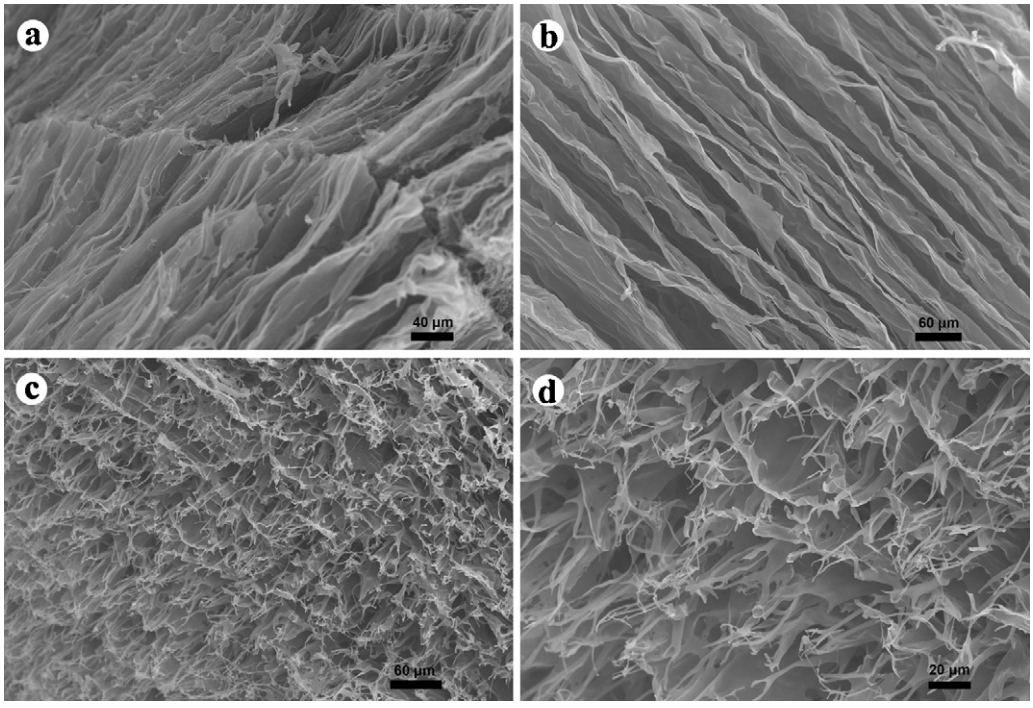

Fig. 6. SEM micrographs of nanofibril foam prepared from the freeze-dried CNs-3.17. (a and b) Micrographs of the cross-section along the aligned direction and (c and d) micrographs of the cross-section with direction perpendicular to fiber alignment.

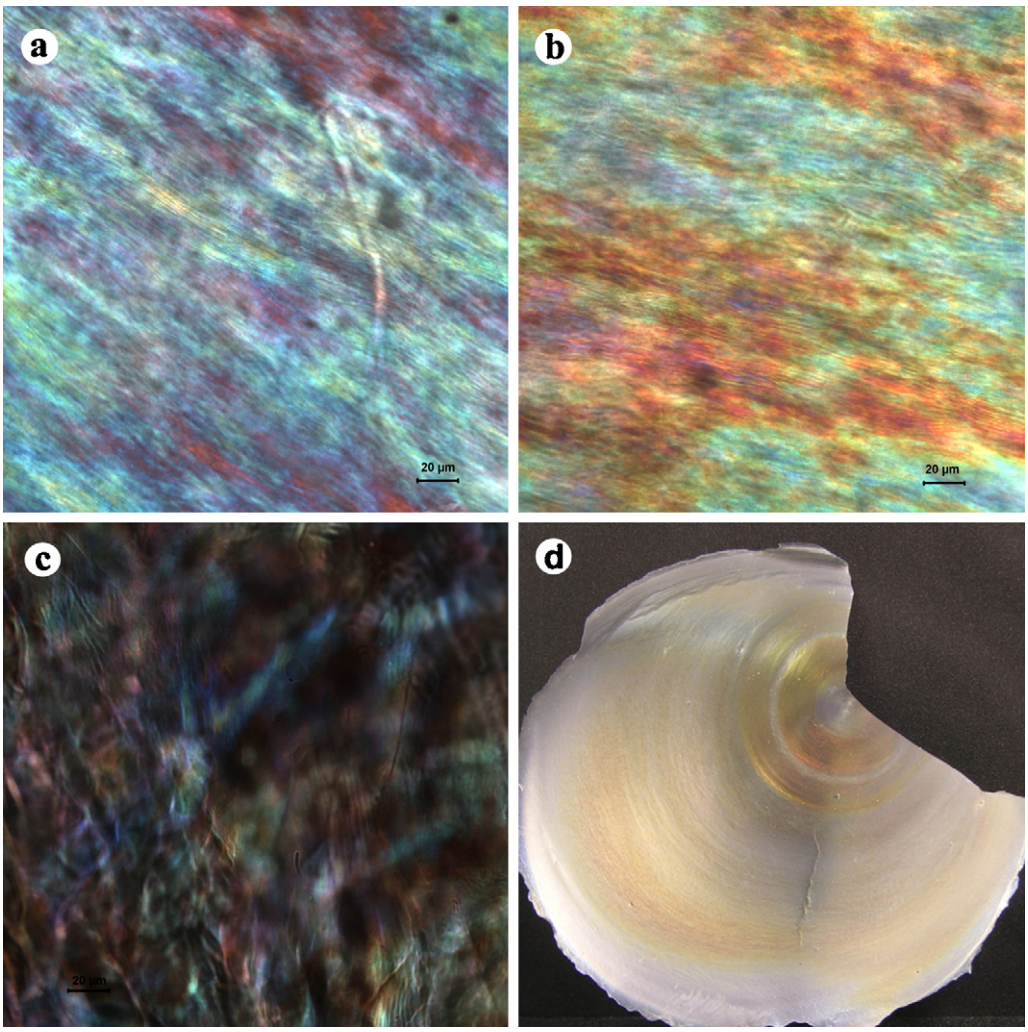

Fig. 7. POM micrographs (a–c) and photo (d) of CNs film. Ordered fingerprints were all shown in liquid crystal phase with iridescent colors.

contributions from the hydrogen bonding interaction and negative ionic interactions among inter- or intra-molecular chains at 35 or 40 °C. Thus, a stronger and compacter gel network was formed at 35 or 40 °C than at other temperatures.

CNs colloids showed a strong concentration dependent behavior resulted from rheology properties. Furthermore, the structure or phase transition of CNs colloids related to concentrations was revealed by polarized optical microscope. Under polarized light, a small block with slightly birefringence as shown in Fig. 5(a) was surrounded by isotropic phase that was randomly oriented in the dilute regime. It was a requirement of the minimization of free energy which could push the CNs spontaneously aligned or self-assembled to produce a high degree of local order leading to anisotropic domain formation. It can be deduced the isotropic–nematic phase transition was assigned to occur when the concentration of CNs was below 0.91%. The sample became progressively more birefringent since the concentration was increased. It is revealed that a microscopic phase separation with coexisting isotropic (nonbirefringent) and nematic (birefringent) phases exhibited in the colloidal suspension of CNs-2.03 (Fig. 5(b)), which is named "I + N" (Gray & Roman, 2006). It is observed that the two nematic phases were aligned along two different directions under polarized light. The CNs-3.17 sample (Fig. 5(c)) was birefringent with colors and clear micro fingerprint, suggesting the presence of cholesteric liquid crystalline phases. It is worth noting that the fingerprint was not aligned along unique direction but twisting (Roman & Gray, 2006). A nematic liquid crystalline alignment was adopted to form an anisotropic phase because of the unidirectional self-orientation of the needle-shaped CNs.

3.3. Microstructure of self-assembled CNs liquid crystal

Fig. 6 shows SEM micrographs of nanofibril foam which was prepared from the freeze-dried CNs-3.17. The foam was composed of many thin membrane layers with width of 1–2 μm, and those membranes compacted layer by layer along the aligned direction as shown in Fig. 6(a) and (b). In fact the membrane layer was composed of oriented nanofibrils when it was observed along the perpendicular to aligned direction (Fig. 6(c) and (d)). These needle-shaped nanofibrils stood out from the broken surface of CNs porous foam. The pores or tubes had diameters varied from 10 to 60 μm and existed between adjacent membrane layers, which meant that cellulose nanofibrils were closely linked with adsorbed and bound water. When water was sublimated from the fibrous network, the foam with ordered, layered, fine micro-sized pore or tube structure was then set up. According to the results from POM tests, the distance between the adjacent fingerprint lines was not equivalent to that of membrane layers measured from SEM. The property of liquid crystal was resulted from the fine and special superstructure of cellulosic nanofibril colloids.

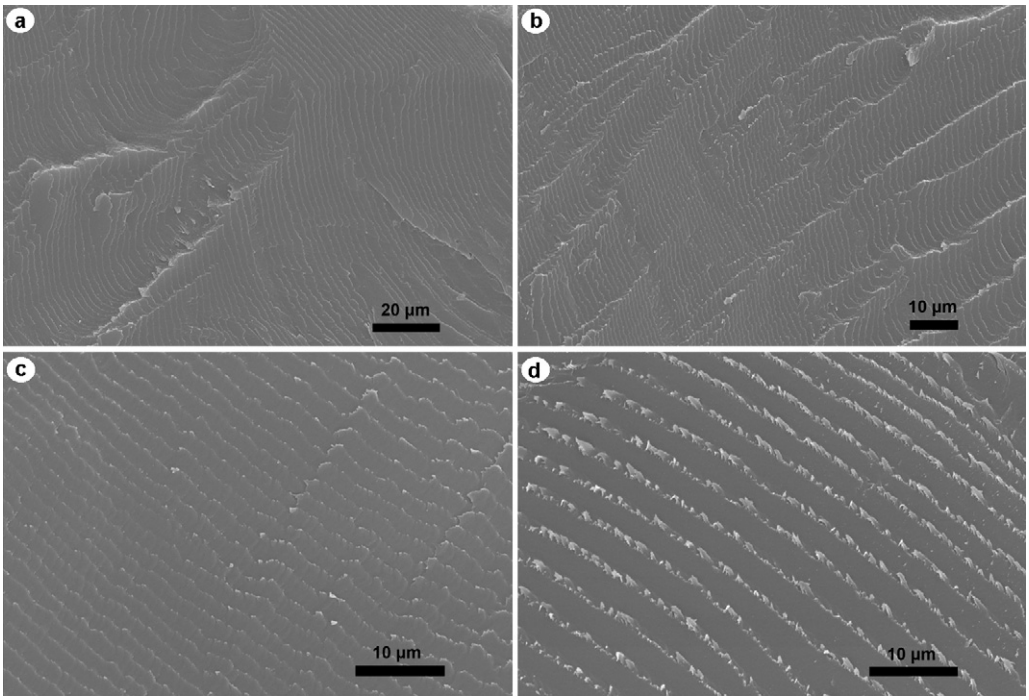

Fig. 8. SEM micrographs of CNs film. (a and b) Micrographs of the cross-section along the aligned direction and (c and d) micrographs of the cross-section with direction perpendicular to fiber alignment.

However, when water was not sublimated but evaporated, the pore or tube structure in the CNs gel networks collapsed, thus leading to compact nanofibril layers. Therefore, the cast CNs sample became a solid film other than porous foam. It is interesting that the film was colored spiraling along the helical axes in as shown in Fig. 7(d). The nature of the color could also be observed by POM shown in Fig. 7(a)–(c). The liquid crystal film exhibited a similar color to the appeared one, and also showed clear ordered fibrous arrangement with a fingerprint. The distance between the adjacent fingerprint is at about 1–2 μm, which is also equivalent to that of in the colloids. It is believed that the period or half pitch for organized nanofibril materials is at about 1–2 μm based on the uniformed cellulose nanocrystals. This structural feature was also seen in the solidified film. Fig. 8 shows the SEM micrographs of broken surface of the CNs film. Many outstanding periodic arches were orderly aligned along a vector direction (Fig. 8(a) and (b)). The distance between the adjacent arches was about 1–2 μm. It was thought that layered fibers were aligned at this direction after one or more periods. From the direction perpendicular to fiber alignment, many protuberances appeared which is accorded to Fig. 6(c) and (d). This is because of the self-alignment of the particles along a vector director in a packed nematic planar such that the angle of the vector director in each subsequent plane is in a spiral stairway packing of nanofibril needles about a cholesteric axis. This period was outside of the range required to reflect visible light, so the film is iridescent because light reflected from the different layers was able to interfere. Therefore, the film exhibits a structural color as a consequence of interference light interaction with a periodic structure, which was found in some insects and plants (Kinoshita, Yoshioka, & Miyazaki, 2008).

4. Conclusions

Uniform cellulose nanocrystals of a needle shape were prepared by the combination of sulfuric acid hydrolysis and high-pressure-homogenization. Crystal lattices of CNs, observed by TEM for the first time, demonstrated the cellulose I structure. When dispersed into water, the homogenized CNs colloids exhibited strong concentration dependence. The flowability became weak caused by increasing concentration. CNs colloid with concentration of 3.17% at 35 °C showed a higher modulus of gel, indicating a compact network which was formed by CNs with strong inter- or intra-molecular interaction at that temperature. With increasing concentration, a liquid crystalline phase was observed in the colloids until complete presentation in the solidified films. It was confirmed that CNs liquid crystal showed ideal fingerprints with period of 1–2 μm, which was corresponded to either the layer width of porous foam or the distance between adjacent periodic arches in the solidified film. This is because of the self-alignment of the CNs along a vector director in a packed nematic planar, and the period of the cholesteric liquid crystalline phases did not change with its state but remained constant. Therefore, the rheology was dependent on the structure and concentration of CNs, whereas the regular period of the ordered liquid crystal phase had no relationship with concentration of CNs but with the nature of CNs, such as, size and surface charge.

Acknowledgements

This work is financially supported by the United States Department of Agriculture CSREES grant (68-3A75-6-508) and National Natural Science Foundation, China.

References

Atalla, R. H., & Vanderhart, D. L. (1984). Native cellulose – A composite of 2 distinct crystalline forms. *Science*, *223*(4633), 283–285.
Beck-Candanedo, S., Roman, M., & Gray, D. G. (2005). Effect of reaction conditions on the properties and behavior of wood cellulose nanocrystal suspensions. *Biomacromolecules*, *6*(2), 1048–1054.
Bercea, M., & Navard, P. (2000). Shear dynamics of aqueous suspensions of cellulose whiskeys. *Macromolecules*, *33*(16), 6011–6016.
Borsali, R., & Gnanou, Y. (2004). On some properties of cellulose rod-like nanocrystals. *Abstracts of Papers of the American Chemical Society*, *227*, U309–U1309.
Dong, X. M., Revol, J. F., & Gray, D. G. (1998). Effect of microcrystallite preparation conditions on the formation of colloid crystals of cellulose. *Cellulose*, *5*(1), 19–32.

Edwards, B. J., & Mchugh, A. J. (1993). A rheooptical study of flow-induced pretransitional ordering in solutions of lyotropic semirigid macromolecules. *Journal of Rheology*, *37*(4), 743–773.
Gardner, K. H., & Blackwel, J. (1971). Substructure of crystalline cellulose and chitin microfibrils. *Journal of Polymer Science Part C: Polymer Symposium*, *36*, 327–340.
Gray, D. G., & Roman, M. (2006). Self-assembly of cellulose nanocrystals: Parabolic focal conic films. *Cellulose Nanocomposites: Processing, Characterization, and Properties*, *938*, 26–32.
Habibi, Y., Lucia, L. A., & Rojas, O. J. (2010). Cellulose nanocrystals: Chemistry, self-assembly, and applications. *Chemical Reviews*, *110*(6), 3479–3500.
Henriksson, M., Henriksson, G., Berglund, L. A., & Lindstrom, T. (2007). An environmentally friendly method for enzyme-assisted preparation of microfibrillated cellulose (MFC) nanofibers. *European Polymer Journal*, *43*(7), 3434–3441.
Kinoshita, S., Yoshioka, S., & Miyazaki, J. (2008). Physics of structural colors. *Reports on Progress in Physics*, *71*, 076401.
Laka, M., Chernyavskaya, S., Treimanis, A., & Faitelson, L. (2000). Preparation and properties of microcrystalline cellulose gels. *Cellulose Chemistry and Technology*, *34*(3-4), 217–227.
Liu, D., Wu, Q., Chen, H., & Chang, P. (2009). Transitional properties of starch colloids with particle size reduction from micro- to nanometer. *Journal of Colloid and Interface Science*, *339*(1), 117–124.
Liu, D., Zhong, T., Chang, P., Li, K., & Wu, Q. (2010). Starch composites reinforced by bamboo cellulosic crystals. *Bioresource Technology*, *101*(7), 2529–2536.
Liu, H., Liu, D., Yao, F., & Wu, Q. (2010). Fabrication and properties of transparent polymethylmethacrylate/cellulose nanocrystals composites. *Bioresource Technology*, *101*(14), 5685–5692.
Marsano, E., Bianchi, E., Boero, E., Gastaldi, G., & Focher, B. (1997). Liquid crystalline polymer gels: Preparation and swelling behavior of cellulase-based networks. *Polymers for Advanced Technologies*, *8*(1), 17–22.
Muller, M., Hori, R., Itoh, T., & Sugiyama, J. (2002). X-ray microbeam and electron diffraction experiments on developing xylem cell walls. *Biomacromolecules*, *3*(1), 182–186.
Nishiyama, Y. (2009). Structure and properties of the cellulose microfibril. *Journal of Wood Science*, *55*(4), 241–249.
Onogi, S., & Asada, T. (1980). G. Astarita, G. Marrucci, & L. Nicolais (Eds.), *Rheology*. New York: Plenum.
Revol, J. F., Godbout, L., & Gray, D. G. (1998). Solid self-assembled films of cellulose with chiral nematic order and optically variable properties. *Journal of Pulp and Paper Science*, *24*(5), 146–149.
Roman, M., & Gray, D. G. (2005). Parabolic focal conics in self-assembled solid films of cellulose nanocrystals. *Langmuir*, *21*(12), 5555–5561.
Roman, M., & Gray, D. G. (2006). Parabolic focal conics in solid films of cellulose nanocrystals. *Abstracts of Papers of the American Chemical Society*, *231*. CELL-099.
Sao, K. P., Samantaray, B. K., & Bhattacherjee, S. (1994). X-ray study of crystallinity and disorder in ramie fiber. *Journal of Applied Polymer Science*, *52*(12), 1687–1694.
Siro, I., & Plackett, D. (2010). Microfibrillated cellulose and new nanocomposite materials: A review. *Cellulose*, *17*(3), 459–494.
Wang, N., Ding, E., & Cheng, R. (2008). Preparation and liquid crystalline properties of spherical cellulose nanocrystals. *Langmuir*, *24*(1), 5–8.
Zimmermann, T., Bordeanu, N., & Strub, E. (2010). Properties of nanofibrillated cellulose from different raw materials and its reinforcement potential. *Carbohydrate Polymers*, *79*(4), 1086–1093.